



**Universiteit Utrecht**

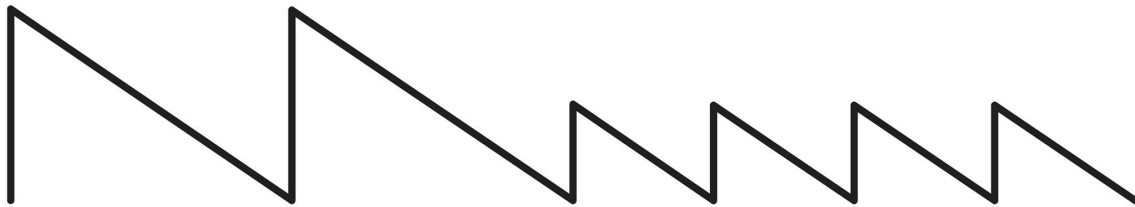


BACHELOR THESIS

---

# Incorporating CO<sub>2</sub> in a three-state climate model

---



*Author:*

Sam Rijken  
Physics & Astronomy  
Studentnr. 3743527  
Utrecht University

*Supervisor:*

dr. Roderik van de Wal  
Utrecht University

15 June 2016



## Abstract

Around one million years ago the dominant frequency of glacial-interglacial cycles shifted from 41 to 100 kyr without apparent changes in insolation forcing. It has been demonstrated this shift, the Mid-Pleistocene Transition, can be simulated with a simple conceptual three-state climate model using only insolation as external forcing, remaining within the framework of classical astronomical theory. In order to produce the Mid-Pleistocene Transition the model uses two linear trends based on the assumption that atmospheric  $\text{CO}_2$  decreased over time. In this research project we will reproduce this model and its results and we will improve the model by removing ad hoc assumptions and replacing the linear trends with continuous  $\text{CO}_2$  forcing.



# Contents

<b>1</b>	<b>Introduction</b>	<b>1</b>
1.1	Mid-Pleistocene Transition . . . . .	1
1.2	Paillard model . . . . .	2
1.3	Research questions . . . . .	4
<b>2</b>	<b>Methods</b>	<b>5</b>
2.1	Data . . . . .	5
2.2	First Paillard model . . . . .	5
2.3	Second Paillard model . . . . .	6
2.4	Third Paillard model . . . . .	7
2.5	Removing truncation and linear trends . . . . .	7
2.6	Incorporating CO <sub>2</sub> . . . . .	8
<b>3</b>	<b>Results</b>	<b>11</b>
3.1	First Paillard model . . . . .	11
3.2	Second Paillard model . . . . .	14
3.3	Third Paillard model . . . . .	16
3.4	Eliminating Paillard trends . . . . .	17
3.5	Incorporating CO <sub>2</sub> . . . . .	18
<b>4</b>	<b>Discussion</b>	<b>23</b>
4.1	Results . . . . .	23
4.2	Conclusion . . . . .	24
4.3	Further research . . . . .	25
4.4	Acknowledgements . . . . .	25
	<b>Bibliography</b>	<b>I</b>
	<b>Python</b>	<b>III</b>



# Chapter 1

## Introduction

On a timescale of hundreds of thousands of years the Earth's climate is characterized by successions of cold and warm periods called glacials and interglacials respectively. In the 1920s, James Croll and Milutin Milankovic constructed a theory of explaining these cycles using only insolation forcing (Petrović, 2009). In this theory, which will be called Milankovic theory from now on, the Earth has three main orbital parameters that determine the amount of radiation the Earth receives from the Sun: precession, obliquity and eccentricity. Precession, the change in the orientation of the Earth's axis, has a periodicity of 23 kyr and is the strongest in terms of spectral power. The second strongest is obliquity, the axial tilt of the Earth, and has a periodicity of 41 kyr. The weakest parameter in terms of spectral power is the eccentricity or non-circularity of the Earth's orbit around the Sun. This eccentricity has a periodicity of approximately 100 kyr, which, quite paradoxically, is the current dominant frequency of the glacial-interglacial cycles in the Earth's climate. It has been said that if Croll and Milankovic knew the dominant frequency of the glacial cycles was 100 kyr they might never have attributed the ice ages to insolation (Muller and MacDonald, 2000, p.232). Since the weakest parameter of Milankovic theory seems to be responsible for the dominant frequency of glacial-interglacial cycles there is thus a discrepancy between theory and observation, known as the 100 kyr-problem. A problem for which many possible solutions have been offered. Amongst these solutions are nonlinear responses to the driving force, amplification of the eccentricity, suppression of the precession and obliquity or even introducing new astronomical parameters such as orbital inclination (Muller and MacDonald, 2000, p.233)(Muller and MacDonald, 1995). However, besides '*failing to reproduce amplitudes and phases of glacial-interglacial cycles*' (Paillard, 1998), these solutions also seem unable to account for a significant interglacial event during a period of small insolation variations around 400 kyr, often called stage 11, and for the Mid-Pleistocene Transition.

### 1.1 Mid-Pleistocene Transition

Whereas the dominant frequency of the glacial-interglacial cycles is now a problematic 100 kyr, it has been 41 kyr (the obliquity frequency) for at least a few million years. However, about one million years ago (between 800 and 1200 kyr before present, BP) the dominant frequency shifted from 41 to 100 kyr and the amplitudes of the glacial-interglacial cycles increased accordingly. This transition is called the Mid-Pleistocene Transition, or MPT, and has been the subject of discussion for decades. The MPT demands an explanation because '*it is [apparently] a singular event and could reflect an unusual occurrence*' (Muller and MacDonald, 2000, p. 253). Explanations based on both astronomical and geological factors have been offered. For example, the orbital inclination model (Muller and MacDonald, 1995) uses a sudden increase in solar system dust (Muller and MacDonald, 2000, p. 253) to increase the amplitudes of the glacial-interglacial cycles. It can be argued, however, that the MPT requires internal changes in climate response because there have been no apparent changes in insolation forcing between 800 and 1200 kyr BP (Daruka and Ditlevsen, 2016).

A topographical cause for these internal changes in climate response could be, for example, slow glacial erosion of the regolith under the Northern-Hemisphere ice sheets (Clark and Pollard, 1998). However, explanations based on topography can only account for a single transition, the MPT. Because it is known more transitions have taken place long before the MPT, solutions based on a slow decrease in atmospheric  $\text{CO}_2$  instead of topographical factors are often preferred. In addition to atmospheric  $\text{CO}_2$ , internal dynamics of ice sheets have been suggested to play a role in explaining the MPT (Bintanja and van de Wal, 2008), but this is beyond the scope of this thesis.

## 1.2 Paillard model

A model that uses the decrease in atmospheric  $\text{CO}_2$  to explain the MPT has been presented by Didier Paillard in his paper ‘The timing of Pleistocene glaciations from a simple multiple-state climate model’ (Paillard, 1998). In the paper he uses a multiple-state representation of the climate system to demonstrate that the 100 kyr-problem, the problematic stage 11 and the MPT can all be solved within the framework of the Milankovic theory. Essentially, Paillard builds a computer model that simulates ice volume using only insolation as external forcing. The model, which will be called the Paillard model from now on, uses three distinct stable climate states called interglacial (i), mild glacial (g) and full glacial (G) and very few tunable parameters that determine when transitions between these states take place (schematic structure in Figure 1.2). These transition parameters, or thresholds, act as the simplest non-linear relation between the insolation forcing and the ice volume. Paillard builds up the model in three stages, each step solving a problem, which will be explained below.

The initial stage, or first Paillard model, is a simple idealized model to determine when transitions between states take place. As mentioned, the climate is assumed to be stable in three regimes: interglacial (i), mild glacial (g) and full glacial (G). The only transitions allowed between these states are from interglacial to mild glacial (i – g), from mild to full glacial (g – G) and from full glacial back to interglacial (G – i). These transitions are governed by two insolation thresholds  $i_0$  and  $i_1$  and an ice volume threshold  $v_{max}$ . The i – g transition is triggered when the insolation falls below the threshold value  $i_0$ , signaling the onset of a cold period of time that allows the ice sheets to start growing. The G – i transition occurs when the insolation rises above  $i_1$ , indicating a period with high temperatures and thus the inception of an interglacial. The g – G transition, from mild to full glacial, will take place when the ice volume exceeds the threshold value  $v_{max}$ . But as there is no explicit ice volume in the first idealized model, the  $v_{max}$  threshold is replaced by a minimal duration  $t_g$  for the g – regime. Physically, this means the mild glacial needs some time to build up its ice volume in order for the transition to a full glacial is possible. An added requirement is that the insolation must remain below a certain insolation value  $i_3$  whilst the mild glacial duration is counted. If the insolation does rise above  $i_3$ , the counter is reset. This enforces the much longer time it takes for ice volume to build up in cold periods than it takes to disappear in warm ones. The graphical representation of this relation is known as a saw tooth wave and is characteristic for ice volume in glacial-interglacial cycles. With this first idealized model a clear 100 kyr glacial-interglacial cycle periodicity is obtained over the past 875 kyr, corresponding with observations and thus offering a solution to the 100 kyr-problem. The details of this simulation are discussed in the Methods section and the outcome is presented in the Results section. An example of the results from the first Paillard model is presented in Figure 1.1.



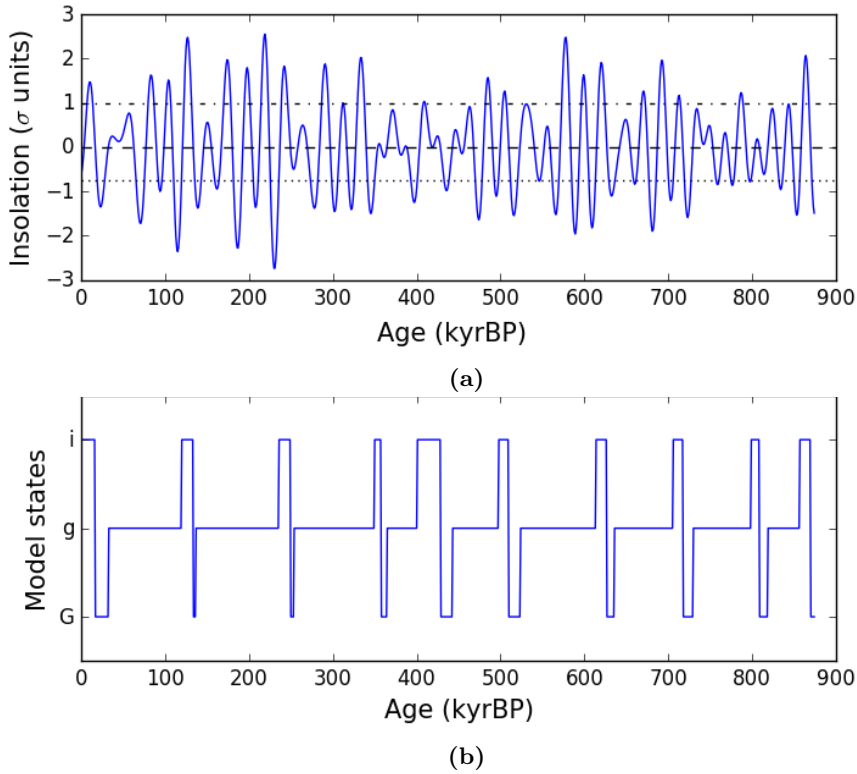


**Figure 1.1 – 1.1a:** Laskar solution for the insolation (blue line),  $i_0 = -0.75$  (dotted line),  $i_1 = i_2 = 0$  (dashed line) and  $i_3 = 1$  (dashdotted line). The minimal duration of a g-regime is  $t_g = 33$  kyr. **1.1b:** Standard results from the first Paillard model, the long interglacial around 400 kyrBP is stage 11.

In the Second Paillard model the ice volume is explicitly represented by a linear differential equation (Equation 2.3.1) with constants depending on the state of the model, resulting in a continuous curve for ice volume. The model thus still needs the three regimes i, g and G to determine the constants for the ice volume equation. The criteria for the i – g and G – i transitions are still the same, determined by the thresholds  $i_0$  and  $i_1$  respectively, but the g – G transitions are now governed by an actual ice volume threshold  $v_{max}$  instead of an artificial counter  $t_g$  that governs the minimum duration of a mild glacial. Each step in time, a new ice volume is computed using the differential equation with the relevant constants and insolation. When the calculated ice volume exceeds this threshold value  $v_{max}$  the mild glacial will become a full glacial. With this second model Paillard demonstrates that the simplest non-linear conceptual model with only insolation forcing as input, in accordance with Milankovic theory, can simulate both the 100 kyr-periodicity of the glacial-interglacial cycles and the problematic stage 11 quite accurately. Again, it is important stage 11 is simulated well because a model based on Milankovic theory should be able to account for such a significant interglacial event during a period of small variations in insolation.

In the third and final Paillard model the range of the simulation is extended to two million years, with thus the Mid-Pleistocene Transition right in the middle. Paillard argues that over this time span slow tectonic activity induces slight topographic changes and a possible decrease in atmospheric  $\text{CO}_2$ . These changes will affect the threshold values of the model and also directly influence the radiative forcing. Paillard represents this with a linearly increasing trend in the ice volume threshold  $v_{max}$ , which influences the timing of the g – G transition, and a linear trend added to the insolation forcing itself. This latter trend physically represents the decrease in atmospheric  $\text{CO}_2$ , a greenhouse gas, and subsequently a decrease in atmospheric temperature. The increasing trend in the ice volume threshold  $v_{max}$  is a result of this linear trend in  $\text{CO}_2$  because the decrease in temperature allows the ice sheets to grow larger in a glacial period.

### 1.3 Research questions

With his linear trends Paillard manages to represent the MPT, but argues a more sophisticated model is needed. The goal of this research project is recreating the Paillard models and improving the final model by replacing the linear trends with a continuous  $\text{CO}_2$  simulation that was not yet available at the time Paillard published his results. The research questions are therefore:

- Can we simulate the Mid-Pleistocene Transition with the three-state climate model as proposed by Paillard?
- Can we improve this model by removing ad hoc assumptions and incorporating continuous  $\text{CO}_2$  forcing?

The methods for answering these questions will be described in the following section, starting with a description of the Paillard model and a formulation for including the  $\text{CO}_2$  forcing over time.

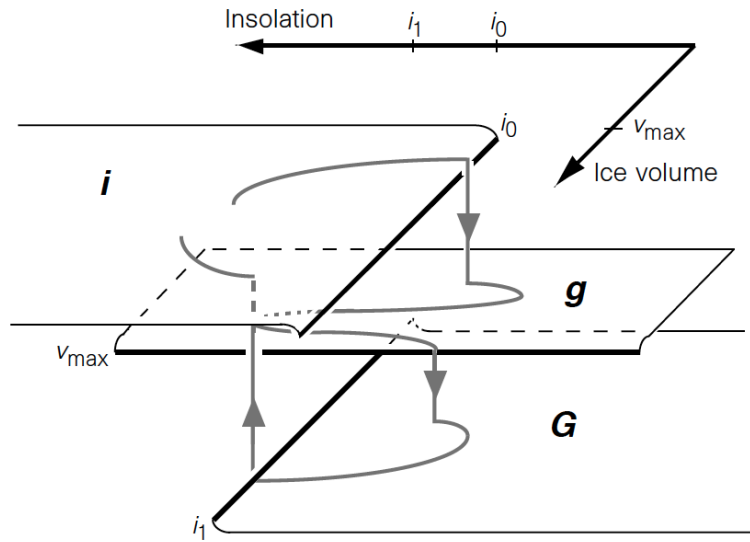


**Figure 1.2** – Structure of the three-state model by Paillard. The climate is assumed to have three regimes: *i*, *g* and *G*. The *i* - *g* transition occurs when the insolation falls below the threshold value  $i_0$ , *g* - *G* occurs when ice volume exceeds  $v_{max}$  and *G* - *i* occurs when the insolation increases above  $i_1$ . In the first model, the  $v_{max}$  threshold is replaced by a minimal duration  $t_g$  for the *g* - regime and the requirement that the previous insolation remains  $i_3$  whilst the model is in the *g* - regime. The *g* - *G* transition then occurs when the insolation decreases below  $i_2$ . In the second model this mechanism is replaced by an actual representation for ice volume, Equation 2.3.1. Figure and description by Paillard (1998)

## Chapter 2

# Methods

### 2.1 Data

All data used in this research project are from the continuous CO<sub>2</sub> simulation by Stap et al. (2016) from which the CO<sub>2</sub> (ppm), sea level (m.s.l.e.) and the June insolation at 65N (W m<sup>-2</sup>) are used. The CO<sub>2</sub> is used for the calculation of a radiation forcing that is added directly to the insolation. This radiation curve will also be projected upon other thresholds, this process is elaborated in Section 2.6. The sea level is inverted and normalized between 0 and 1 to create a reference ice volume that will be used to compare model results to. The insolation, which is the Laskar solution for the June insolation at 65N (Laskar, 1990), is normalized to unit variance and zero mean. This is the only external input data for the Paillard models. Paillard uses the Berger solution for the insolation in the first two models (Berger, 1978) and the Laskar solution for his final model (Laskar, 1990). Because this is quite inconsistent we apply the Laskar solution in all models, as it is used by Stap et al. to generate sea level and CO<sub>2</sub> records. All models are built with the Python programming language.

### 2.2 First Paillard model

This idealized model will determine the climate states as a function of insolation. First, the insolation is normalized to unit variance and zero mean. Depending on the threshold values for insolation transitions will take place between states. The i – g transition occurs when the insolation falls below  $i_0$ . The g – G transition will occur when the insolation falls below  $i_2$ , but the duration of the mild glacial (g) must be at least  $t_g$  during which the insolation cannot rise above  $i_3$ . If the insolation does rise above  $i_3$  the counter for  $t_g$  is reset. The G – i transition occurs when the insolation rises above  $i_1$ . The threshold values are  $i_0 = -0.75$ ,  $i_1 = i_2 = 0$ ,  $i_3 = 1$ ,  $t_g = 33$  kyr and the initial state is a full glacial (G) at 875 kyrBP. These threshold values are in variance units and are empirically defined by Paillard to place the transitions at the right point in time. He argues that the thresholds are not very sensitive to changes, different values will only slightly offset the transitions by a few hundred years but the overall shape will remain the same. (Paillard, 1998)

Once the model is set up the parameters are allowed to vary individually in order to check and quantify the sensitivity of the model as reported by Paillard. The parameter changes are restricted by the conditions that the end state at present day is an interglacial, and that the model has 9 glacial cycles in the whole range of 875 kyr. If these conditions appear insufficient in the sense that some glacial cycles become very misplaced relative to the initial result, additional conditions about the timing of sensitive glacial cycles are added. Ambiguous statements made by Paillard such as ‘*changes are minor*’ and ‘*not very sensitive*’ are then defined more objectively.

Finally, a small hypothesis about the reset-function of  $t_g$  will be tested. When the model is in a mild glacial and the insolation rises above  $i_3$ , the timer that counts the time the model is in the mild glacial is abruptly reset to 0. Physically, this implies that the ice volume disappears (almost) entirely within one temporal resolution step of 1000 years. Instead of this hard reset, it is more realistic to count down with  $t = t - 2$  for every point in time the insolation is above  $i_3$ , with the obvious condition that  $t_g$  may not become negative. Physically, this represents a rapid decline of the ice volume instead of a sudden disappearance. If the result of the model is unchanged or still satisfactory according to the conditions used for the sensitivity experiments, the sensitivity experiments will be repeated with this new condition for  $t_g$ . This approach is physically more realistic than the hard reset, but no further conclusions will be drawn as the entire mechanism is replaced by actual ice volume calculations in the next models.

### 2.3 Second Paillard model

In the second model the ice volume is allowed to change continuously, but it still uses the three climate regimes. The i – g transition again occurs when the insolation falls below  $i_0$  and the G – i transition also occurs when the insolation rises above  $i_1$ . However, the g – G transition is now triggered by the ice volume exceeding a threshold value  $v_{max}$  rather than by a time scale  $t_g$ . Ice volume is determined by the linear differential equation:

$$\frac{dv}{dt} = (v_R - v)/\tau_R - F/\tau_F \quad (2.3.1)$$

where  $v$  is the ice volume, (subscript)  $R$  refers to the current climate regime being i, g or G,  $v_R$  is the reference ice volume for the different regimes,  $F$  is the forcing,  $\tau_F$  and  $\tau_R$  are time constants. The time constant  $\tau_F$  can be interpreted as a state-independent time scale associated to the heat capacity of the ice sheets, the  $\tau_R$  values are state-dependent timescales for the ice volume in different climate states (Ashwin and Ditlevsen, 2015). In the model with  $\text{CO}_2$  incorporated, the constraint that  $\tau_g = \tau_G$  is used because there should be no reason why the ice sheets would grow at different rates in the mild or full glacial. Also, order of magnitude 1 difference between the glacial and interglacial timescales is preferred because, in general, a glacial period lasts approximately 100 kyr while the interglacial ablation takes about 10 kyr. Paillard does not seem to use this last constraint but he does coincidentally also use  $\tau_g = \tau_G$ . The threshold values chosen by Paillard in this model are  $v_{max} = 1$ ,  $i_0 = -0.75$  and  $i_1 = 0$ . The constants are  $v_g = v_G = 1$ ,  $v_i = 0$ ,  $\tau_g = \tau_G = 50$  kyr,  $\tau_i = 10$  kyr,  $\tau_F = 25$  kyr. In this second Paillard model, the forcing that is used for the calculation of ice volume is a ‘*smoothed truncation*’ of the insolation, calculated with the function:

$$F = \frac{1}{2} \left( x + \sqrt{4a^2 + x^2} \right) \quad (2.3.2)$$

where  $x$  is the insolation and  $a$  is the truncation parameter. This adjustment ‘*accounts for the lower sensitivity of the ice volume during colder periods*’ (Paillard, 1998). The truncation is calculated by first normalizing the insolation to unit variance and zero mean, then applying the truncation function and then normalizing to unit variance and zero mean again. Although this truncation (Equation 2.3.2) is used to reproduce the results by Paillard, it will be eliminated from the final model as it is physically rather arbitrary to adjust the forcing itself rather than the model formulation that uses this forcing to calculate an ice volume. Instead it appears as a model deficiency, and we show that it is possible to obtain good results without this seemingly ad hoc empirical adjustment to the forcing itself. The insolation data with and without truncation ( $a = 1$ ) is presented in Figure 2.1 below.

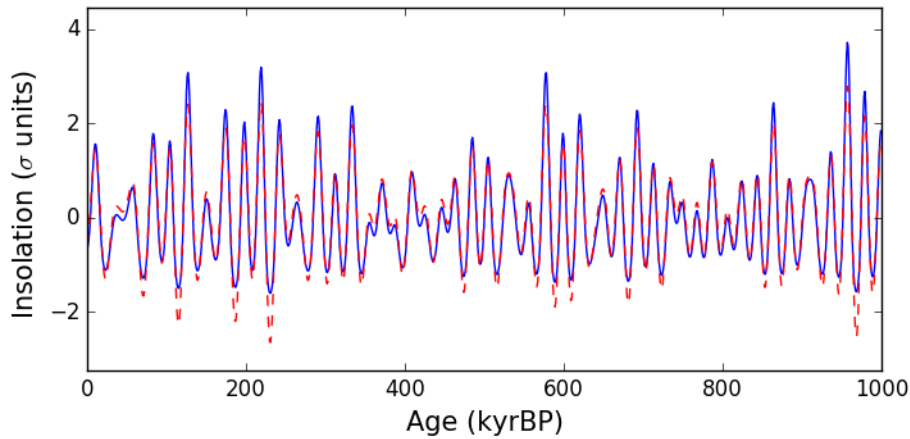


**Figure 2.1** – Insolation before (red dashed line) and after truncation (blue line) for  $a = 1$ .

The initial conditions for the simulation are an ice volume  $v_0 = 0.75$  in a mild glacial (g) state, starting at 1 MyrBP. Sensitivity experiments are carried out by varying the parameters individually, keeping the rest constant. Again the constraints are that the end state at present day must be an interglacial and the model needs to give exactly 10 glacial cycles in this period of 1 Myr. This time however, Paillard also indicates that stage 21 (850 kyrBP), stage 19 (780 kyrBP) and stage 3 (40 kyrBP) are ‘*particularly sensitive*’. These will thus also become a constraint and need to be correctly positioned in time for a parameter value to be accepted.

## 2.4 Third Paillard model

In the final model Paillard switches to the Laskar solution for the insolation forcing. The threshold conditions, normalization and truncation remain the same but the period of the simulation is extended to the past 2 million years and two linear trends are introduced: a linearly increasing  $v_{max}$  value from 0.35 to 1.1, as a function of time, and a (quite large) trend of  $3 \text{ W m}^{-2} \text{ Myr}^{-1}$  added to the radiative forcing before all the normalization and truncation, thus starting with an added  $6 \text{ W m}^{-2}$  two million years ago. The ice volume constants remain the same as in the second Paillard model, but the time constants are now  $\tau_g = \tau_G = 80 \text{ kyr}$ ,  $\tau_i = 5 \text{ kyr}$ ,  $\tau_F = 28 \text{ kyr}$ . The truncation parameter  $a = 1$ . No explanation for the changes in parameter values is given by Paillard so we must assume these were empirical adjustments. The initial conditions are now an ice volume  $v_0 = 0.35$  in a mild glacial (g) state, starting at 2 MyrBP. There will be no sensitivity experiments carried out on this simulation for two reasons: Paillard has not done so either, leaving me with no results to compare to, and the  $\text{CO}_2$  is incorporated in the model with different parameter values.

## 2.5 Removing truncation and linear trends

As a measure to test model performance we use a root mean square error (RMSE) between model results and the reference ice volume. First the RMSE directly between the forcing, normalized between 0 and 1, and the reference ice volume (both by Stap et al., 2016) is calculated to see if the model results after incorporation of continuous  $\text{CO}_2$  are actually an improvement on Milankovic theory. Also the RMSE between the result from the third Paillard model and the reference ice volume is calculated. This enables us to quantify the improvements made by the model with incorporated  $\text{CO}_2$  (Table 3.3).

Because Paillard’s third model is mainly dependent on the truncation and linear trends, his parameter values  $v_{max}$ ,  $i_0$ ,  $i_1$ ,  $\tau_G$ ,  $\tau_g$ ,  $\tau_i$  and  $\tau_F$  stop producing the best model results after the elimination of these factors. Therefore new parameter values have to be found.

Furthermore, because  $\tau_g$  and  $\tau_G$  should be equal from a physical perspective,  $\tau_G$  will also become  $\tau_g$  in the differential equation for the ice volume (Equation 2.3.1). We are thus left with only two different timescales  $\tau_R$ :  $\tau_g$  for mild and full glacial,  $\tau_i$  for interglacial. New values for the remaining parameters  $v_{max}$ ,  $i_0$ ,  $i_1$ ,  $\tau_g$ ,  $\tau_i$  and  $\tau_F$  need to be found. This is achieved by assigning a list of possible values to these parameters and calculating the root mean square error (RMSE) between the model results of all possible combinations of parameter values with the reference ice volume. The lowest possible RMSE is then selected, essentially allowing the model to choose its own parameter values, and the associated constant values will be checked to see if there is any reason to disagree with them physically. The range of the simulation for determining the constants is limited to a starting point at 574 kyrBP where the sea level is at a minimum, effectively at 0. This point in time is chosen because a similar sea level minimum occurs at 2020 kyrBP, allowing the tuning of the parameters and the start of the simulation to be with the same initial conditions:  $v_0 = 0$  in an interglacial (i). The model is tested for all possible combinations of the following lists:

$$\begin{aligned} v_{max} &= \{0.4, 0.6, 0.8, 0.9, 1.0, 1.1\} \\ i_0 &= \{-1.1, -1, -0.9, -0.8, -0.75, -0.7, -0.6, -0.5, -0.4\} \\ i_1 &= \{-0.9, -0.8, -0.7, -0.6, -0.5, -0.4, -0.3, -0.2, -0.1\} \\ \tau_i &= \{5, 6, 7, 8, 9, 10, 11, 12, 13, 14\} \\ \tau_g &= \{40, 45, 50, 55, 60, 65, 70, 75, 80, 85, 90\} \\ \tau_F &= \{24, 25, 26, 27, 28, 29, 30, 31, 32, 33, 34\} \end{aligned}$$

These values are chosen because they include all values Paillard used, and everything in between. If the model prefers a minimum or maximum allowed value, the parameter space is widened. If it prefers a value in the middle of the list, additional possibilities around this value are included. A root mean square error is calculated if there are precisely six i – g transitions in the simulation (the six known glacial cycles in the past 574 kyr) and the end state in present day is an interglacial. When a set of optimal parameters has been obtained, they will all be allowed to vary individually so the sensitivity of the model can be investigated. With these optimal parameter values in hand, the starting point of the simulation will then be extended to the reference ice volume minimum at 2020 kyrBP. The model will then run without any trends, linear or continuous, to show that the dominating frequency of the result is 100 kyr over the entire range.

## 2.6 Incorporating CO<sub>2</sub>

Initially, the continuous CO<sub>2</sub> simulation (Stap et al., 2016) will be incorporated in the same way Paillard did. This implies adding a trend directly to the forcing and coupling this trend to the ice volume threshold  $v_{max}$ , allowing it to increase over time. This time, however, the trends will not be linear but continuous because they are calculated directly from the CO<sub>2</sub> simulation. The values added to the radiative forcing are calculated with:

$$\Delta R = 5.35 \cdot \ln \left( \frac{\text{CO}_2}{\text{CO}_{2,0}} \right) \quad (2.6.1)$$

where  $\text{CO}_{2,0} = 278$  ppm (Köhler et al., 2012). A linear fit of this curve will then be made and the present-day value of this fit will be added to the entire  $\Delta R$ -curve, causing the linear fit of the resulting curve to become 0 on present day. This is done in order to be consistent with the trends postulated by Paillard as much as possible (a decreasing linear trend added to the forcing, ending with 0 radiation added at present day).

The increasing threshold value  $v_{max}$  that determines the g – G transition will then be coupled to this  $\Delta R$  because, when the  $v_{max}$  is influenced by the decreasing trend in CO<sub>2</sub>, it might also be influenced by its fluctuations. This coupling is achieved by first creating a straight line from a starting value  $v_{max,2020}$ , which is the  $v_{max}$  threshold value at 2020 kyrBP, to a final value  $v_{max,0}$ , the  $v_{max}$  value at present day. In Paillard’s model

this line increases from 0.35 (at 2000 kyrBP) to 1.1 without giving an explicit reason besides obtaining a satisfying result. Here the model will be allowed to choose its own preferred values again. In order to project the  $\Delta R$  curve upon this straight line, first the difference between the  $\Delta R$  curve and its linear fit is calculated for every moment in time. This creates a data-set of *deviation from the linear fit*. A new parameter  $S_{v_{max}}$  is then introduced, representing the sensitivity of the  $v_{max}$  threshold to the  $\Delta R$  variations. This  $S_{v_{max}}$  is multiplied to the deviation from the linear fit and the resulting curve is then added to the straight line for  $v_{max}$ . An example of  $\Delta R$  and  $v_{max}$  curves is presented in Figure 2.2 for the values  $v_{max,0} = 1.1$ ,  $v_{max,2020} = 0.35$  and  $S_{v_{max}} = 0.1$ .

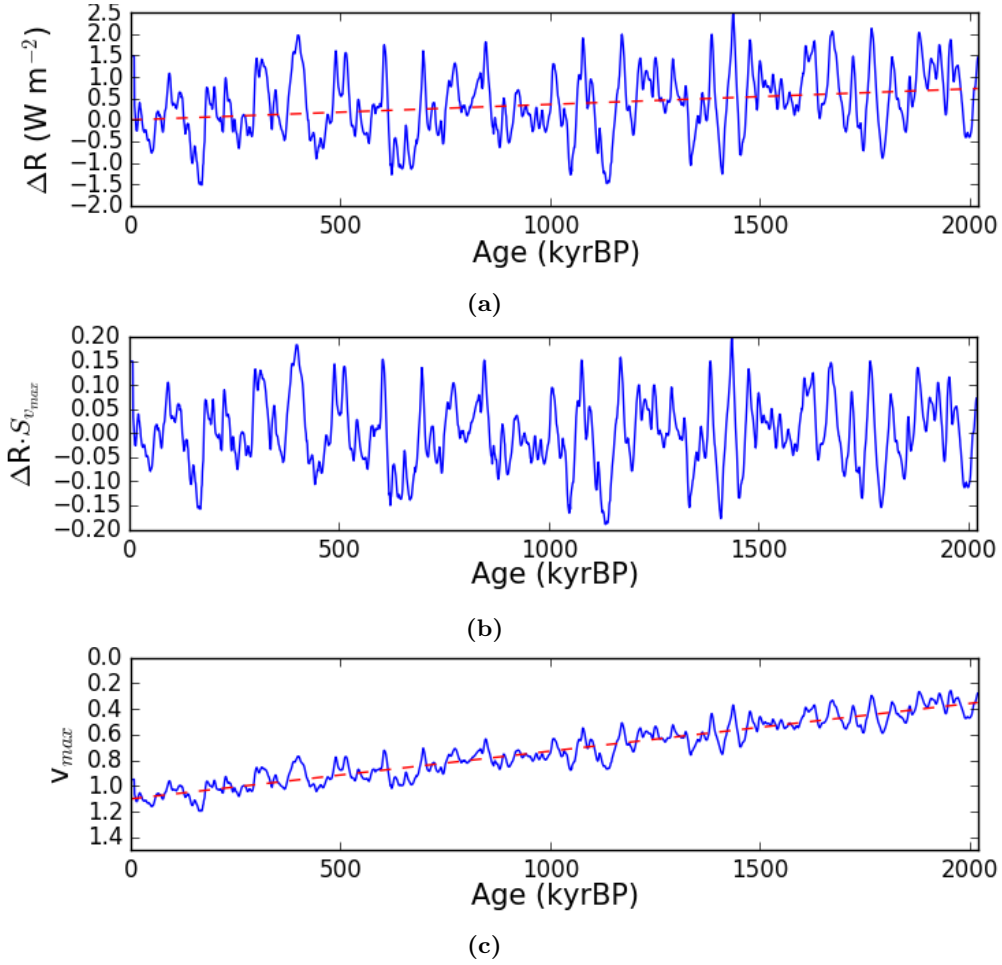


**Figure 2.2** – An example of determining the continuous  $v_{max}$  threshold curve. **2.2a**: The radiation added directly to the forcing (blue line) and its linear fit (red dashed line). **2.2b**: The deviation from the linear fit multiplied by  $S_{v_{max}} = 0.1$ . **2.2c**: The  $v_{max}$  curve (blue line) and its linear fit (red dashed line), with  $v_{max,0} = 1.1$ ,  $v_{max,2020} = 0.35$  and  $S_{v_{max}} = 0.1$ .

All allowed parameter values are:

$$\begin{aligned}
 v_{max,0} &= \{0.6, 0.7, 0.75, 0.8, 0.85, 0.9, 0.95, 1.0, 1.05, 1.1, 1.15, 1.2\} \\
 v_{max,2020} &= \{0, 0.05, 0.1, 0.15, 0.2, 0.25, 0.3, 0.35, 0.4, 0.45, 0.5, 0.55, 0.6\} \\
 S_{v_{max}} &= \{-0.3, -0.2, -0.1, 0.0001, 0.05, 0.1, 0.15, 0.2, 0.25, 0.3, 0.35, 0.4, \\
 &\quad 0.5, 0.6, 0.7, 0.8, 0.9, 1\}
 \end{aligned}$$

As shown in the lists above, the  $v_{max}$  threshold is allowed to start anywhere between 0 and 0.6 at 2020 kyrBP and may increase to anywhere between 0.6 and 1.2 at present day. An  $S_{v_{max}}$  of 0.0001 leaves us with just the linear trend as all the  $\Delta R$  influences have been multiplied by effectively zero (a non-zero value is chosen to avoid any multiplication issues). A negative value represents a reverse influence on the ice volume threshold by the decreasing  $\text{CO}_2$  and thus  $\Delta R$ , this would contradict the increasing linear trend but the model is given the possibility anyway just to account for all possibilities. As it is hard, not to say impossible, to quantify in advance how strongly the  $v_{max}$  threshold should react to the deviations in  $\Delta R$ , the sensitivity parameter  $S_{v_{max}}$  is allowed values up to 1. This value would mean the  $\Delta R$  curve is projected directly upon the linear trend for  $v_{max}$ , which is probably much too strong as the standard deviation in the  $\Delta R$  curve is most likely equal to or larger than the difference between  $v_{max,2020}$  and  $v_{max,0}$ .

All possible combinations of these parameter values are tried by the model and, if the final state is an interglacial, again a root mean squared error with the reference ice volume is calculated in order to find the combination of values that gives the lowest possible RMSE and thus the best fit. Then the three parameters  $v_{max,0}$ ,  $v_{max,2020}$  and  $S_{v_{max}}$  will again be allowed to change individually in order to investigate the sensitivity of the model, this time using the RMSE as a constraint.

Finally, the threshold values  $i_0$  and  $i_1$  that were constant in all Paillard's models are also allowed to vary according to the continuous  $\text{CO}_2$  simulation. This is done in the same way as the  $v_{max}$  curve is obtained. For example, the  $i_0$  curve is determined by first creating a straight line from a starting value  $i_{0,2020}$  at 2020 kyrBP to a final value  $i_{0,0}$  at present day. Then again a sensitivity parameter is introduced, called  $S_{I_0}$  this time, and multiplied to the same deviation from linear fit of the  $\Delta R$  as used for  $v_{max}$ . The resulting curve is then added to the straight line, resulting in a curve coupled to the  $\text{CO}_2$ . This process is exactly the same for  $i_1$ . There is no explicit motivation for allowing these parameters  $i_0$  and  $i_1$  to vary according to  $\text{CO}_2$  besides checking if statistically more accurate results can be obtained by doing this. The lists of allowed values are:

$$\begin{aligned}
 i_{0,0} &= \{-0.3, -0.4, -0.5, -0.6, -0.7, -0.8\} \\
 i_{0,2020} &= \{0, -0.1, -0.2, -0.3, -0.4, -0.5\} \\
 i_{1,0} &= \{-0.3, -0.4, -0.5, -0.6, -0.7, -0.8\} \\
 i_{1,2020} &= \{0, -0.1, -0.2, -0.3, -0.4, -0.5\} \\
 S_{i_0} &= \{-0.15, -0.1, -0.05, 0.0001, 0.05, 0.1, 0.15\} \\
 S_{i_1} &= \{-0.15, -0.1, -0.05, 0.0001, 0.05, 0.1, 0.15\}
 \end{aligned}$$



## Chapter 3

# Results

### 3.1 First Paillard model

The results for the first Paillard model are presented in Figure 3.2b. Whereas the model seems to be functioning well, the results are not exactly the same as those obtained by Paillard because of the different insolation datasets. The differences between the Laskar and Berger solution for the insolation forcing (both for June, 65N) are small, but they become apparent now because some differences lie around the threshold values. Two of these differences are marked in Figure 3.1. We can see the insolation rises above the zero-mean average at 356 kyrBP and thus above  $i_1$ . This allows the model to make a transition from full glacial (G) to interglacial (i). In the Berger solution used by Paillard, the insolation does not rise above  $i_1$  and the model remains in the full glacial stage for quite some time. Also, the maxima at 845 and 825 kyrBP do not rise above the threshold value  $i_3$ . Because the model is in a mild glacial here, the timer  $t_g$  that restricts the model from making a transition to a full glacial is not reset and a premature g – G transition, and consequently a G – i transition, is allowed. Albeit slightly different from Paillard’s graph, Figure 3.2b clearly demonstrates the Laskar solution also provides a satisfactory result. Interestingly, the minor adaptation of the  $t_g$  reset ( $t = t - 2$  instead of  $t = 0$  when  $i > i_3$  in a mild glacial) does not change the placement of any transition. The only influence it has on the graph with standard settings for parameters is a slight lengthening of the full glacials around 250 and 625 kyrBP (Figure 3.2c). The results for the sensitivity experiments are presented in Table 3.1.

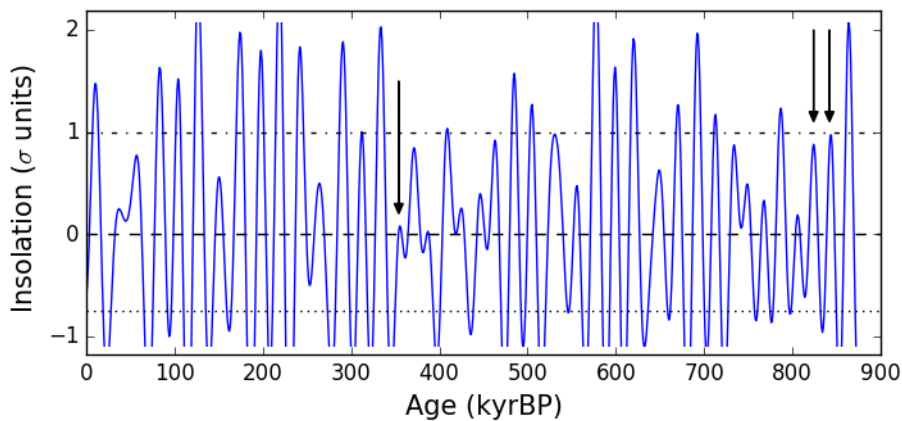


**Figure 3.1** – Marked differences in insolation with Berger solution (arrows), Laskar solution for the insolation (blue line),  $i_0 = -0.75$  (dotted line),  $i_1 = i_2 = 0$  (dashed line) and  $i_3 = 1$  (dashdotted line).

The ranges for the parameter values as shown in Table 3.1 are obtained by allowing the parameters to vary individually and checking to see when the model fails to meet the conditions mentioned in the Methods section. Where starting in a full glacial, as prescribed by Paillard, gives an extra glaciation period between 850 and 875 kyrBP, all other periods are completely unaffected by the starting state. Paillard might have experienced the misplacement of the first two transitions because of his different insolation, most notably his insolation rising above  $i_3$  at 825 kyrBP which causes the mild-glacial counter to reset. Below  $i_0 = -0.86$  we lose a full cycle around 700 kyrBP, above  $i_0 = -0.61$  the end state will change to a mild glacial. We see that for both x and y, the results remain unchanged. When  $i_1$  is chosen below -0.20, the end state jumps to a mild glacial. This is because the threshold is so low that the full glacial will immediately change to an interglacial, but this happens whilst the insolation is still below  $i_0$ , which in turn immediately causes the interglacial to change into a mild glacial again. Remarkably  $i_1$  can be set as high as 1.03 in our model, only then the glaciation period around 400 kyrBP (stage 11) will be significantly changed. Yet again, the reason for the deviation from Paillard's results could be the different insolation: our insolation rises above the zero mean precisely at this moment whilst Paillard's insolation does not. The threshold for  $i_2$  can be as low as -0.50 because only for  $i_2 < -0.50$  does the insolation-minimum at 250 kyrBP not reach this threshold anymore, causing the model to skip the transition to a full glacial and thus a full period. Again, Paillard's insolation seems to have a minimum at -0.30 at 250 kyrBP, which creates his low-boundary for  $i_2$ . Any value for  $i_2$  above 0.12 will result in a mild glacial at present day.

The lower boundary for  $i_3$  is the same as Paillard reports, below 0.97 a glacial period is lost at 550 kyrBP. Until now the two criteria that have been used seemed reasonable and sufficient, but problems started to arise at the upper boundary for  $i_3$ : until 1.63 indeed 9 full periods and an interglacial at present day are obtained, but especially the glacial period at 250 kyrBP is very misplaced. This raises the argument that the position of a few well-known glaciation cycles should also be a constraint on the boundaries. If we take the position of the glacial cycle at 250 kyrBP as a constraint as well, the upper boundary would be  $i_3 = 1.22$ , which is in much better agreement with Paillard. Until then the results are exactly the same as the unchanged model results, but for  $i_3 = 1.23$  the glacial cycle that should be at 250 kyrBP happens way too early. It is puzzling why Paillard would have such a high value of  $t_g = 60$  as his upper boundary for  $t_g$ : the mild glacial at 150 kyrBP clearly has no time to build up its ice volume because of the many high insolation maxima when  $t_g > 35$  kyr.

The only significant difference between the results of x and y is for the allowed variations in  $i_3$  and  $t_g$ . These two are now more restricted because glacial cycles are displaced more easily, mostly the interglacial at 330 kyrBP occurring way too early. Also the next two cycles, at 250 and 125 kyrBP, are easily displaced relative to the standard result because of the high insolation peaks. The lower boundary of  $i_2$  also becomes a bit lower: for  $-0.79 < i_3 < -0.62$  the full glacials above 250 and 800 kyrBP are slightly delayed but it could be argued that they are still in agreement with the data and they do meet the criteria. Since the differences between x and y are not major and the entire mechanism with  $t_g$  is replaced by actual ice volume in the next model, this case will be given no further attention. In short, there are no major differences between the results by Paillard besides the much higher upper boundary for  $t_g$  reported by Paillard. The other (minor) differences are all due to insolation differences.

**Table 3.1** – Allowed parameter values for the first idealized model. Results for the unchanged model and the model with the changed condition for  $t_g$  are named x and y, respectively.

Variable	Paillard's results	(x) Results	(y) Results $t = t - 2$ for $i > i_3$
Starting state	i, g, G	i, g, G	i, g, G
$i_0$	$-0.97 < i_0 < -0.64$	$-0.87 < i_0 < -0.61$	$-0.87 < i_0 < -0.61$
$i_1$	$-0.23 < i_1 < 0.32$	$-0.20 < i_1 < 1.04$	$-0.20 < i_1 < 1.04$
$i_2$	$-0.30 < i_2 < 0.13$	$-0.51 < i_2 < 0.13$	$-0.79 < i_1 < 0.13$
$i_3$	$0.97 < i_3 < 1.16$	$0.97 < i_3 < 1.22$	$0.67 < i_3 < 1.03$
$t_g$ (kyr)	$27 < t_g < 60$	$20 < t_g < 35$	$31 < t_g < 35$

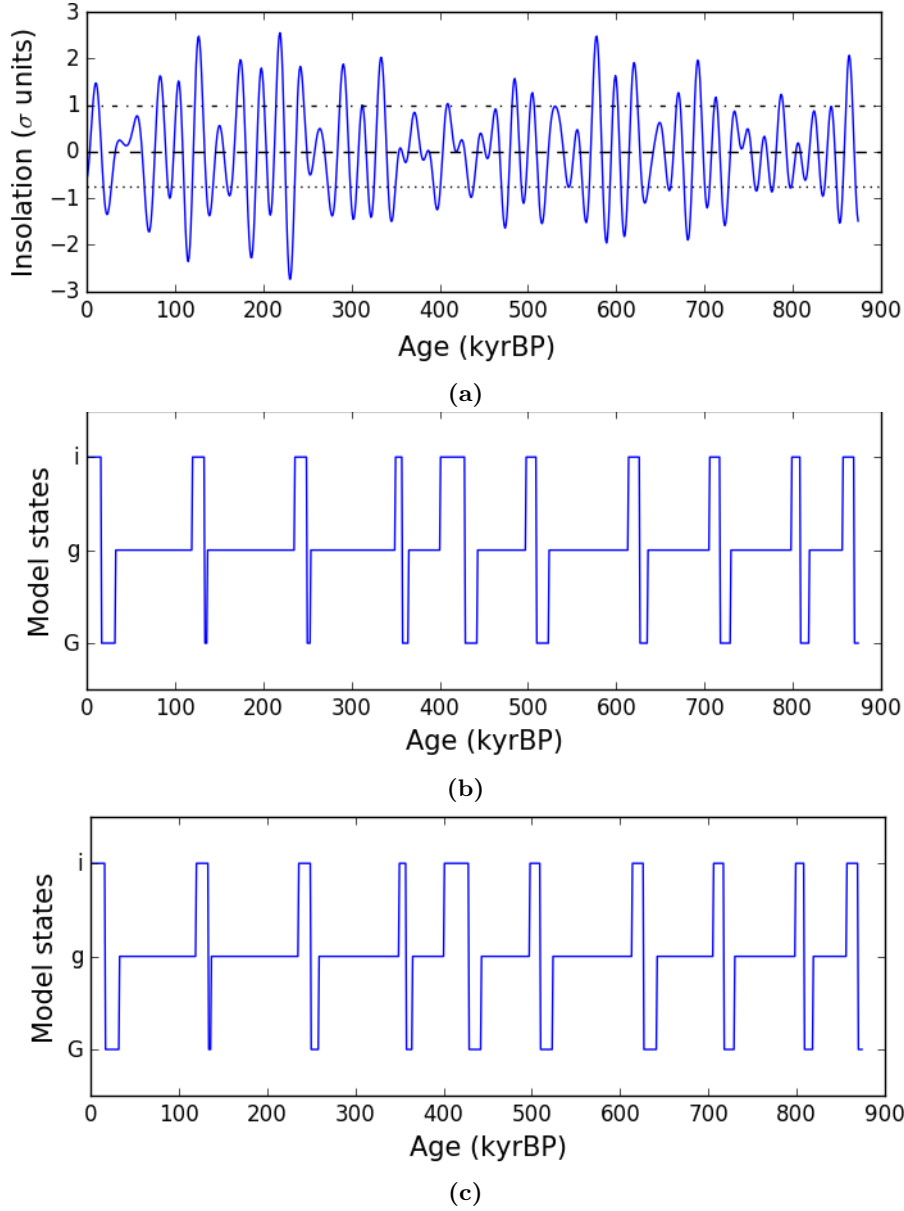


**Figure 3.2** – **3.2a**: Laskar solution for the insolation (blue line),  $i_0 = -0.75$  (dotted line),  $i_1 = i_2 = 0$  (dashed line) and  $i_3 = 1$  (dashdotted line). **3.2b**: Standard results from the first Paillard model,  $t_g = 33$  kyr. **3.2c**: Results from the first Paillard model with  $t = t - 2$  instead of  $t = 0$  when  $i > i_3$  in a mild glacial.

## 3.2 Second Paillard model

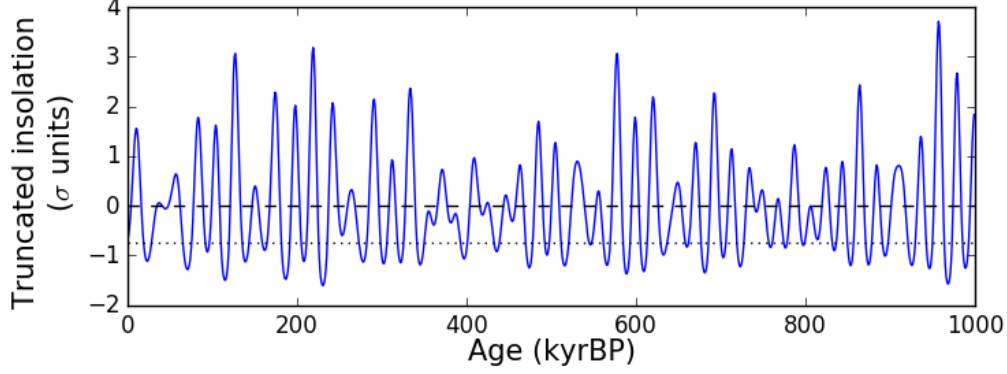
In Figure 3.3 we see the results from the reproduction of Paillard’s second model. Due to the slight differences in insolation, a minimum truncation parameter  $a = 1.21$  is needed for the ice volume to increase enough for the first cycle to appear at around 950 kyrBP and the next cycle at 890 kyrBP to match the result by Paillard (Figure 3.3b). This is because the initial state is a mild glacial, and the ice volume needs low insolation to increase above 1 for the model to make a g – G transition. Too much truncation,  $a = 1$ , will prevent the model from doing so (Figure 3.3c). Once the model is in a full glacial and the insolation rises above  $i_1$ , the G – i transition will occur and the first cycle is complete. The result now appears to be very much in agreement with the result Paillard obtains, probably because the differences between the Laskar and Berger solutions for the insolation have been smoothened out by the truncation. The sensitivity results are presented in Table 3.2.

Just like in model 1 our model is less sensitive to the starting state than Paillard’s model. Starting in both interglacial and mild glacial gives the exact same result, starting in a full glacial changes only the position of the first cycle. At  $\tau_G = 0.4$  the results will start to change, at  $\tau_G = 0.3$  the criteria will not be met anymore. But since our resolution is on the order of 1 kyr and  $\tau_G = 1$  still meets the criteria the bottom boundary will be presented as larger than zero, just like Paillard does. Logically, a value between 0 and 1 for the time constants can mess up the differential equation for the ice volume (Equation 2.3.1). The criteria will indeed still be met for any value of  $\tau_G$  above the default 50. For  $\tau_g$  values of 41 and lower all three criteria simultaneously fail, but this is only because stage 3 has become an interglacial. At  $\tau_g > 51$  we already lose the interglacial period at 950 kyrBP but this is because our truncation is at the highest possible level to barely allow this interglacial, so every change to the ice volume will make it disappear. From  $\tau_g = 64$  onwards, however, we also lose the interglacial at 120 kyrBP. For  $\tau_i > 16$  the transition at 720 kyrBP will occur much too early but the criteria are still met, for  $\tau_i > 20$  the criteria will fail as we have an extra cycle between 400 and 600 kyrBP. Between  $\tau_F$  values of 21 and 22 the conditions are still met but the interglacial at 520 kyrBP becomes anomalous, below 21 we get an extra cycle between 300 and 500 kyrBP. For  $\tau_F > 26$  we lose the first interglacial again, probably due to the truncation. Also the next interglacial at 870 kyrBP loses its ice volume minimum, but this is arguably more in agreement with the data. From  $\tau_F = 40$  onwards stage 3 changes significantly again, causing the model to end in a mild glacial.

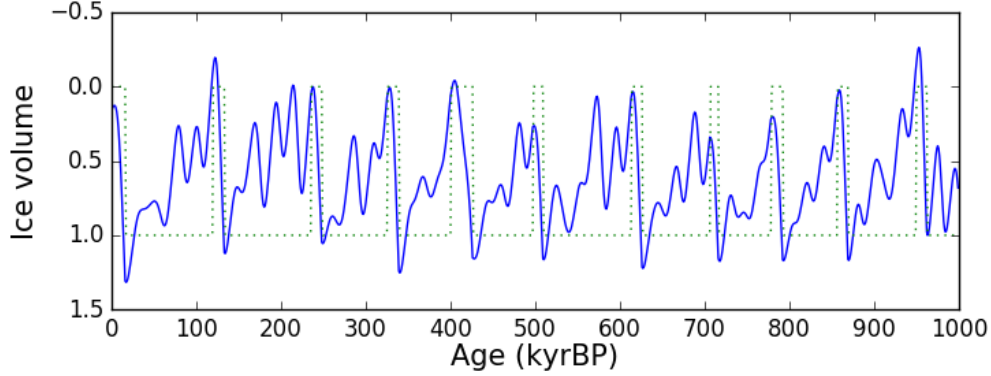
The only significant difference with Paillard’s results is in the truncation parameter. For any value below 1.21 the first interglacial at 950 kyrBP will be lost, therefore  $a = 1.21$  is chosen as default (Figure 3.3b). Remarkably,  $a$  can be chosen as high as 3.09 without any change in cycles. Only for  $a > 3.09$  will stage 3 become interglacial again, changing the end state to a mild glacial. For  $a$  approaching infinity we experience more change in the result than just stage 7.3 and 3 becoming interglacial, as reported by Paillard, because also stage 13 (510 kyrBP) essentially skips the full glacial stage where the ice volume exceeds  $v_{max} = 1$  and immediately goes to an interglacial ice volume minimum.

**Table 3.2** – Allowed parameter values for the second Paillard model.

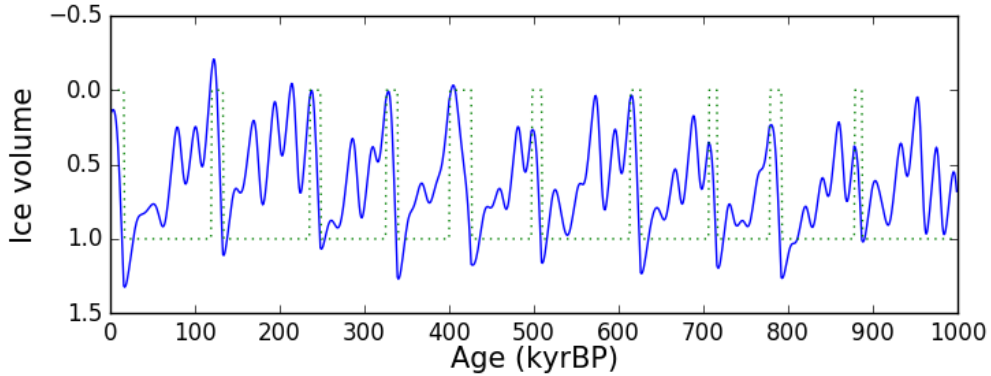
Variable	Paillard's results	Results
Starting state	i, g, G	i, g, G
$\tau_G$ (kyr)	$0 < \tau_G < \text{infinity}$	$0 < \tau_G < \text{infinity}$
$\tau_g$ (kyr)	$47 < \tau_g < 57$	$41 < \tau_g < 64$
$\tau_i$ (kyr)	$0 < \tau_i < 20$	$0 < \tau_i < 15$
$\tau_F$ (kyr)	$23 < \tau_F < 29$	$20 < \tau_F < 40$
$a$	$0.54 < a < 1.66$	$1.20 < a < 3.10$



(a)



(b)

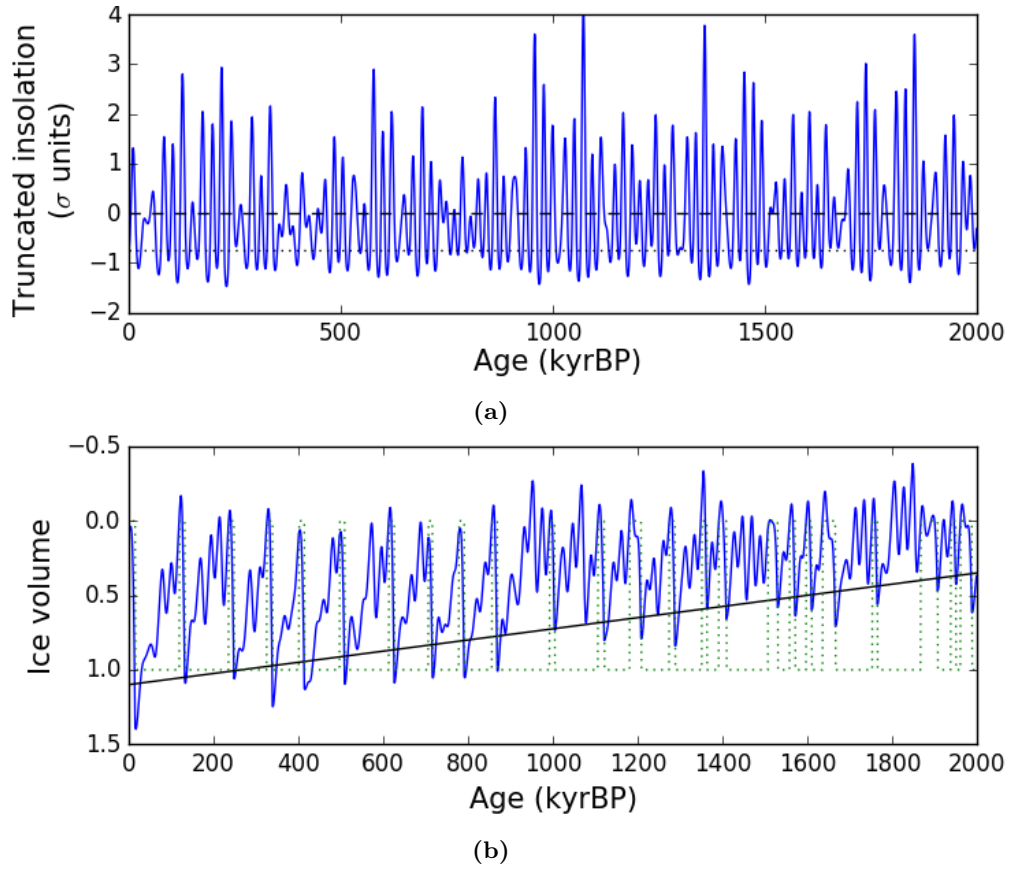


(c)

**Figure 3.3** – **3.3a**: Truncated insolation with  $a = 1$  (blue line),  $i_0 = -0.75$  (dotted line) and  $i_1 = 0$  (dashed line). **3.3b**: Results from the second Paillard model with  $a = 1.21$  (blue line) and  $v_R$  (green dotted line), where 0 is interglacial and 1 is mild or full glacial. The constants are  $v_g = v_G = 1$ ,  $v_i = 0$ ,  $\tau_g = \tau_G = 50$  kyr,  $\tau_i = 10$  kyr,  $\tau_F = 25$  kyr. **3.3c**: Results from the second Paillard model with  $a = 1$ , the first interglacial is lost.

### 3.3 Third Paillard model

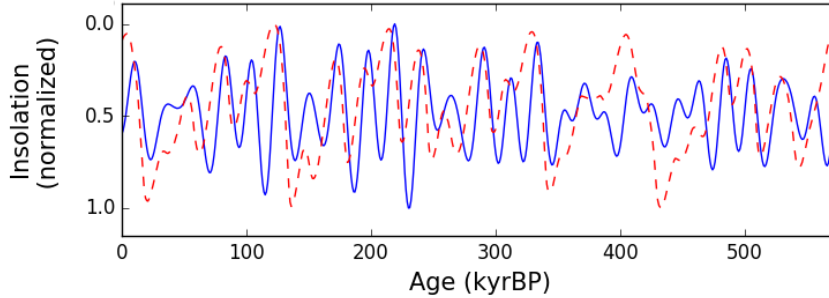
This last Paillard model does indeed simulate the Mid-Pleistocene Transition around 0.9 – 1 MyrBP, showing a clear transition from 40-kyr to 100-kyr glaciation cycles (Figure 3.4). For this simulation, Paillard switched from the Berger to the Laskar solution for the insolation without changing his parameter values. As we are now both working with the same insolation curve the truncation parameter is changed back to  $a = 1$ . The root mean square error between the calculated ice volume and reference ice volume (obtained by inverting the sea level data by Stap et al., 2016), both normalized between 0 and 1, is  $\text{RMSE} = 0.15025$ . This value will be used to compare results from models with incorporated  $\text{CO}_2$  with (Table 3.3).



**Figure 3.4** – 3.4a: Truncated insolation (blue line) with the truncation parameter  $a = 1$ ,  $i_0 = -0.75$  (dotted line), and  $i_1 = 0$  (dashed line). 3.4b: Results from the third Paillard model (blue line), the  $v_{max}$  threshold (black line) increasing linearly from 0.35 to 1.1 and  $v_R$  (green dotted line), where 0 is interglacial and 1 is mild or full glacial. The constants are  $v_g = v_G = 1$ ,  $v_i = 0$ ,  $\tau_g = \tau_G = 80$  kyr,  $\tau_i = 5$  kyr,  $\tau_F = 28$  kyr.

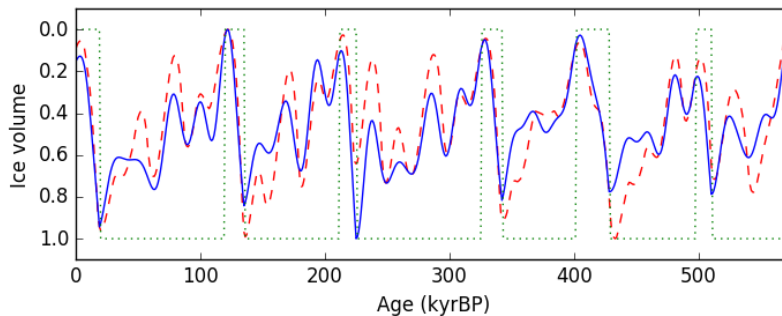
### 3.4 Eliminating Paillard trends

Figure 3.5 shows the normalized insolation *without truncation* plotted directly against the reference ice volume for the last 574 kyrBP, resulting in a  $\text{RMSE} = 0.26761$ . This will thus be the reference RMSE value, no higher RMSE between model results and reference ice volume is accepted when parameters are tested.



**Figure 3.5** – Calculating the RMSE directly between insolation (blue line), normalized between 0 and 1, and reference ice volume (red dashed line).  $\text{RMSE} = 0.26761$ .

For the last 2020 kyrBP, the range for simulations with incorporated  $\text{CO}_2$ , the root mean square error becomes  $\text{RMSE} = 0.29245$ . This value will be used to quantify improvements made by models with incorporated  $\text{CO}_2$  (Table 3.3). Now the model was run between 574 kyrBP and present day for all possible combinations of parameter values given in the Methods chapter and a RMSE was calculated if the result met the conditions also given in the Methods chapter. The obtained new parameter values are  $v_{\max} = 0.8$ ,  $i_0 = -0.6$ ,  $i_1 = -0.9$ ,  $\tau_i = 11$ ,  $\tau_g = 80$ ,  $\tau_F = 34$  (Figure 3.6). These were then allowed to vary individually, plotting the resulting RMSE against the possible values. Interestingly, there appeared to be only 1 possible value for the variables  $v_{\max}$ ,  $\tau_i$ ,  $\tau_g$  and  $\tau_F$ . It appears that removing the truncation has also removed some flexibility of the model, however still providing a proper result. The threshold  $i_0$  could vary between -0.8 and -0.6 with the RMSE remaining almost constant,  $i_1$  was allowed between -0.9 and -0.4. Physically,  $i_1$  should be as high as possible because this determines when the G – i transition takes place. A low value for  $i_1$  would mean the model can enter an interglacial stage when the insolation is still very low. However, for the model to be in an interglacial at present day the parameter  $i_1$  must be equal to or lower than  $i_0$ . This results in the final parameter values  $v_{\max} = 0.8$ ,  $i_0 = -0.6$ ,  $i_1 = -0.6$ ,  $\tau_i = 11$ ,  $\tau_g = 80$ ,  $\tau_F = 34$ . Extending the range of the simulation to 2020 kyr indicates a constant amplitude and 100-kyr periodicity throughout the entire range (Figure 3.7). This would be expected for the model without (linear) trends.



**Figure 3.6** – The optimal model result without trends and truncation for the last 574 kyr (blue line), the reference ice volume (red dashed line) and  $v_R$  (green dotted line). Here  $\text{RMSE} = 0.135$  for  $v_{\max} = 0.8$ ,  $i_0 = -0.6$ ,  $i_1 = -0.9$ ,  $\tau_i = 11$ ,  $\tau_g = 80$ ,  $\tau_F = 34$ .



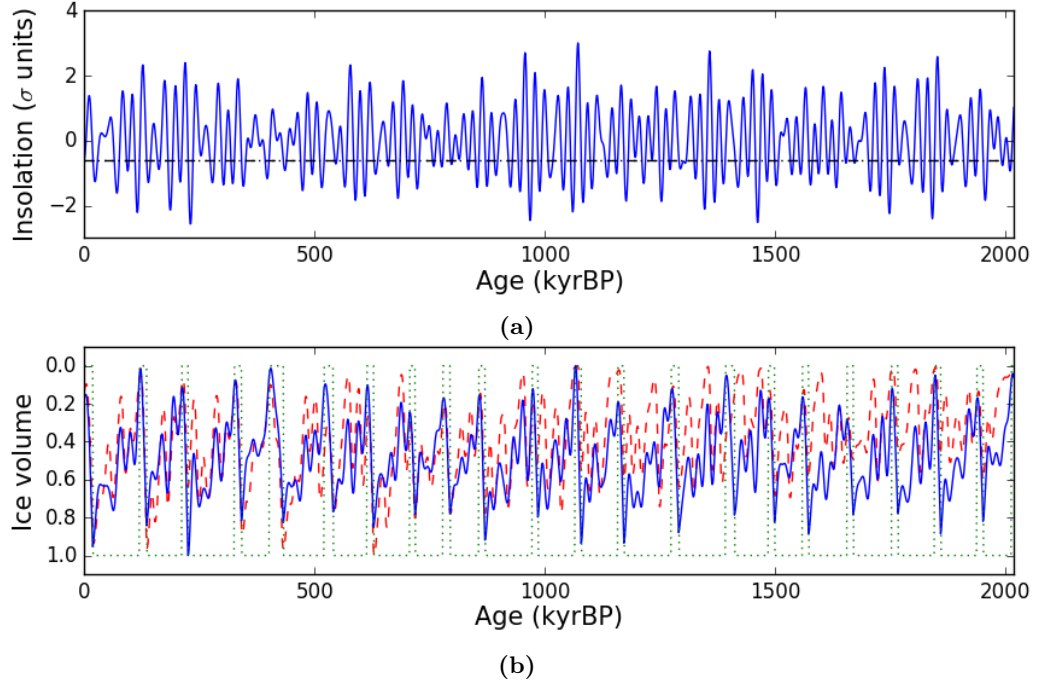


**Figure 3.7** – **3.7a**: Insolation without truncation (blue line) and  $i_0 = i_1 = -0.6$  (dashed line). **3.7b**: Results for the model without trends and truncation (blue line), reference ice volume (red dashed line) and  $v_R$  (green dotted line), where 0 is interglacial and 1 is mild or full glacial. The constants are  $v_{max} = 0.8$ ,  $i_0 = -0.6$ ,  $i_1 = -0.6$ ,  $\tau_i = 11$ ,  $\tau_g = 80$ ,  $\tau_F = 34$ .

### 3.5 Incorporating CO<sub>2</sub>

In Figure 3.8 we see the model results with incorporated trends in  $v_{max}$  and the forcing, dependent on the continuous CO<sub>2</sub> simulations. The model-runs resulted in one clear minimum RMSE = 0.14690 for the parameter values  $v_{max,2020} = 0.5$ ,  $v_{max,0} = 0.9$  and  $S_{v_{max}} = 0.0001$ , implying the model is very sensitive to parameter changes but able to provide a good result. The onset of the 100-kyr periodicity is correctly placed at around 1 MyrBP, but the transition seems more gradual than in the linear trend simulation by Paillard. This may very well not be a bad thing because, aside from the initial 100 kyr, the placement of all minima and maxima seems to be in harmony with the reference ice volume. It is however very peculiar that although the model does want a linear trend in the  $v_{max}$  threshold, which corresponds to the overall decrease in CO<sub>2</sub>, it does not accept fluctuations in  $v_{max}$  by demanding an  $S_{v_{max}}$  of effectively zero. However, when linear trends in the insolation thresholds  $i_0$  and  $i_1$  are allowed (Figure 3.9) the sensitivity parameter for the  $v_{max}$  threshold becomes a non-zero value  $S_{v_{max}} = 0.1$  and the CO<sub>2</sub> fluctuations thus appear in the  $v_{max}$  curve. The best result now has a root mean square error of RMSE = 0.13981 for the parameter values  $i_{0,2020} = -0.2$ ,  $i_{0,0} = -0.6$ ,  $i_{1,2020} = i_{0,0} = -0.4$ ,  $v_{max,2020} = 0.35$ ,  $v_{max,0} = 0.85$  and  $S_{v_{max}} = 0.1$ . This is an improvement compared to the RMSE = 0.14690 of the model results without linear trends in the insolation thresholds  $i_0$  and  $i_1$  (Table 3.3). The improvement is mainly because the modelled ice volumes in the interglacial-glacial cycles between 600 and 420 kyrBP and the interglacial period around 1000 kyrBP are now much more in agreement with the reference ice volume. There are also some changes in the first 200 kyr of the simulation but the main improvement is in the two aforementioned cycles. Interestingly, only the  $i_0$  threshold decreases linearly while  $i_1$  remains constant. When these insolation thresholds are then also allowed to fluctuate according to the CO<sub>2</sub> curve (Figure 3.10), along with the  $v_{max}$  fluctuations,  $i_1$  still remains constant on  $i_0 = -0.4$  and the minor fluctuations in the  $i_0$  caused by its sensitivity parameter now becoming  $S_{i_0} = -0.05$  have very little effect



on the modelled ice volume. Only the initial 200 kyrBP change slightly, after which the model returns to its previous results. The sensitivity parameter needs a negative number because it is an inverse trend compared to the  $v_{max}$  threshold, whilst the  $v_{max}$  increases and needs a positive projection of the CO<sub>2</sub> curve the  $i_0$  threshold decreases and thus also needs an inverse relation. When the sensitivity parameter for  $i_0$  is chosen a slightly stronger  $S_{i_0} = -0.1$  the amplitudes of the cycle around 900 kyrBP become anomalous while the rest of the simulation remains the same, indicating strongly localized change with respect to parameter changes.

In short, incorporating a continuous CO<sub>2</sub> curve in the trends introduced by Paillard decreases the root mean square error with reference ice volume from RMSE = 0.15025 to RMSE = 0.14690, an improvement of only 2.2 %, both nearly halving the RMSE directly between the normalized forcing and reference ice volume. Another decrease in RMSE from 0.14690 to 0.13981, an improvement of 4.8 %, is obtained when the insolation thresholds  $i_0$  and  $i_1$  are also allowed linear trends. Incorporating CO<sub>2</sub> in these insolation trends to allow fluctuations has very little effect on the other parameters and the root mean square error with the reference ice volume, as the  $v_{max}$  parameters remain the same and the RMSE is only improved by another 0.8 %. In total, allowing the insolation and ice volume thresholds to fluctuate according to CO<sub>2</sub> decreases the root mean square error between the model results and reference ice volume from 0.15025 to 0.13867, an improvement of 7.7 %.

**Table 3.3** – RMSE between model results and reference ice volume for the past 2020 kyr.

<i>Model</i>	<i>RMSE</i>
Milankovic	0.29245
Paillard	0.15025
CO <sub>2</sub> ( $v_{max}$ , forcing)	0.14690
CO <sub>2</sub> ( $v_{max}$ , forcing) Linear $i_0$ and $i_1$	0.13981
CO <sub>2</sub> ( $v_{max}$ , forcing, $i_0$ , $i_1$ ) $S_{i_0} = -0.1$	0.13872
CO <sub>2</sub> ( $v_{max}$ , forcing, $i_0$ , $i_1$ ) $S_{i_0} = -0.05$	0.13867

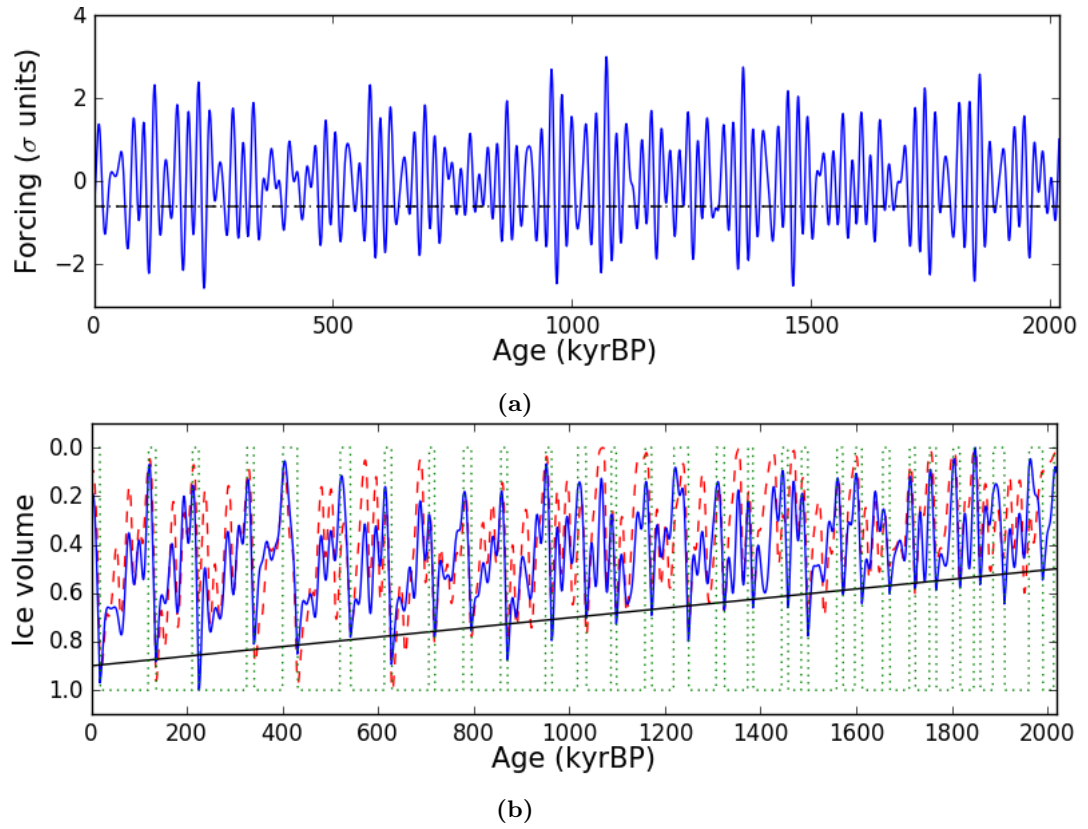


**Figure 3.8 – 3.8a:** Insolation with added  $\Delta R$  forcing (blue line) and the thresholds  $i_0 = i_1 = -0.6$  (dashed line). **3.8b:** Model results with incorporated  $\text{CO}_2$  trends (blue line), reference ice volume (red dashed line),  $v_R$  (green dotted line) and the  $v_{max}$  curve (black dashed line). The constants are  $\tau_i = 11$ ,  $\tau_g = 80$ ,  $\tau_F = 34$ ,  $i_0 = -0.6$ ,  $i_1 = -0.6$ ,  $v_{max,2020} = 0.5$ ,  $v_{max,0} = 0.9$  and  $S_{v_{max}} = 0.0001$ .

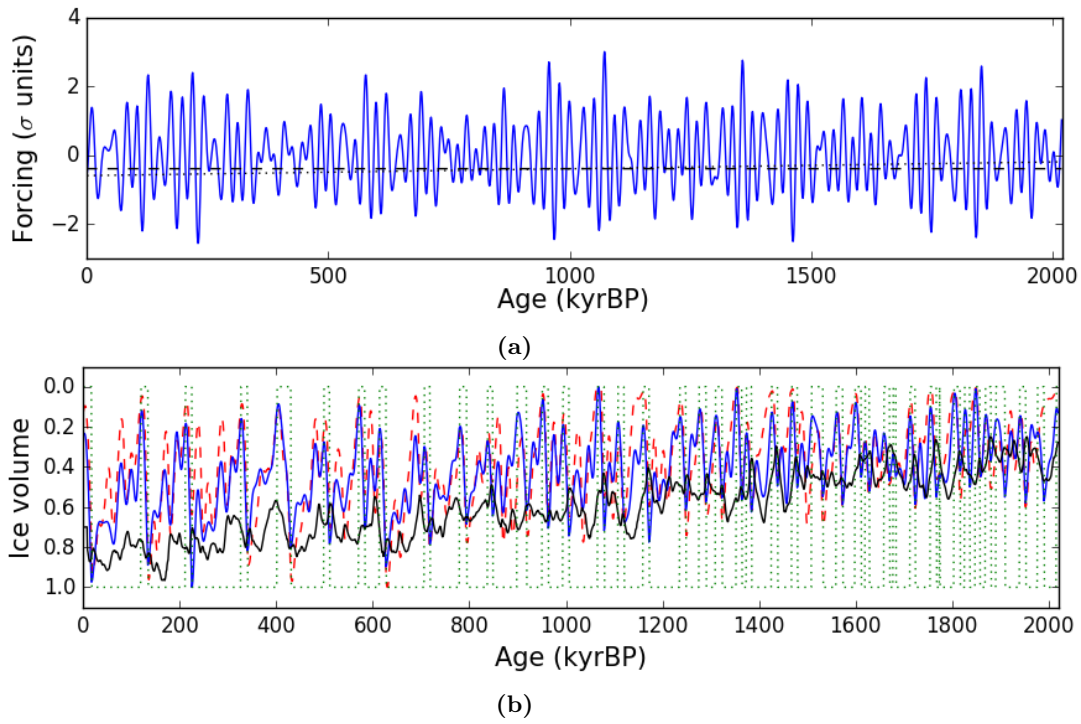


**Figure 3.9 – 3.9a:** Insolation with added  $\Delta R$  forcing (blue line),  $i_1 = -0.4$  (dashed line) and  $i_0$  decreasing linearly from  $-0.2$  to  $-0.6$  (dotted line). **3.9b:** Model results with incorporated CO<sub>2</sub> trends (blue line), reference ice volume (red dashed line),  $v_R$  (green dotted line) and the  $v_{max}$  curve (black dashed line). The constants are  $\tau_i = 11$ ,  $\tau_g = 80$ ,  $\tau_F = 34$ ,  $i_{0,2020} = -0.2$ ,  $i_{0,0} = -0.6$ ,  $i_{1,2020} = i_{0,0} = -0.4$ ,  $v_{max,2020} = 0.35$ ,  $v_{max,0} = 0.85$  and  $S_{v_{max}} = 0.1$ .

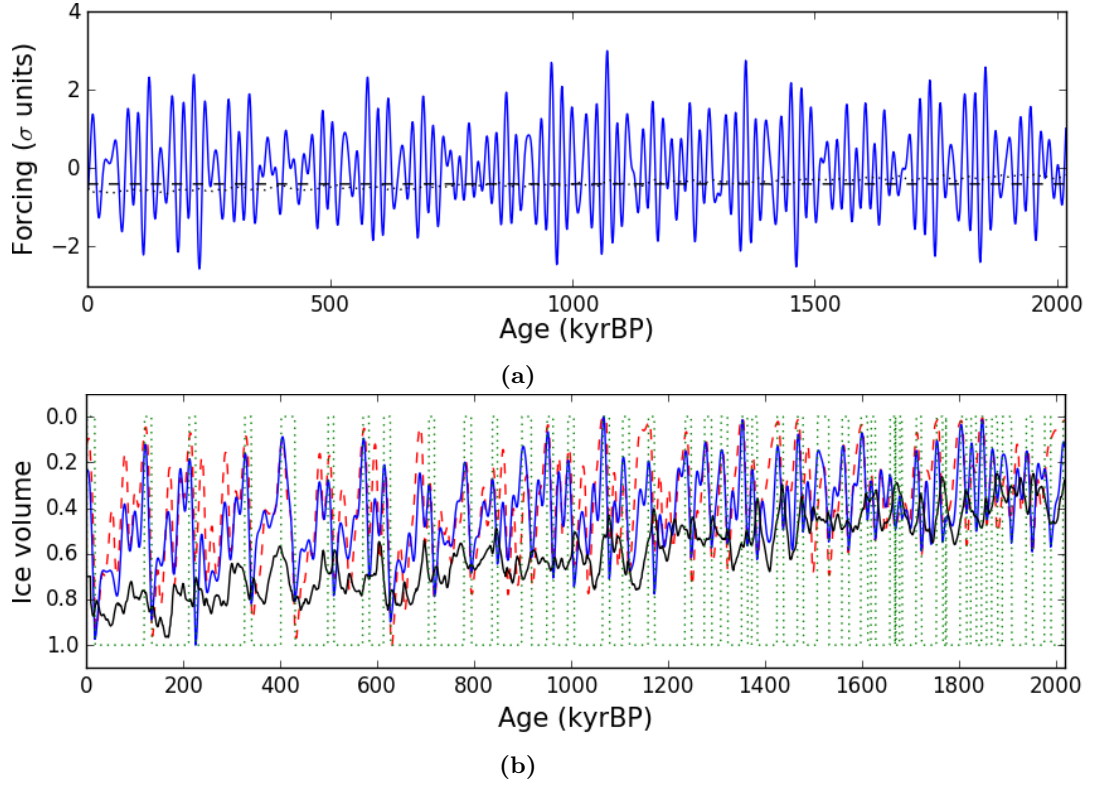


**Figure 3.10 – 3.10a:** Insolation with added  $\Delta R$  forcing (blue line),  $i_1 = -0.4$  (dashed line) and the  $i_0$  curve decreasing from  $-0.2$  to  $-0.6$ , now fluctuating according to CO<sub>2</sub>, with  $S_{i_0} = -0.05$  (dotted line). **3.10b:** Model results with incorporated CO<sub>2</sub> trends (blue line), reference ice volume (red dashed line),  $v_R$  (green dotted line) and the  $v_{max}$  curve (black dashed line). The constants are  $\tau_i = 11$ ,  $\tau_g = 80$ ,  $\tau_F = 34$ ,  $S_{i_0} = -0.05$ ,  $i_{0,2020} = -0.2$ ,  $i_{0,0} = -0.6$ ,  $i_{1,2020} = i_{0,0} = -0.4$ ,  $v_{max,2020} = 0.35$ ,  $v_{max,0} = 0.85$  and  $S_{v_{max}} = 0.1$ .

## Chapter 4

# Discussion

### 4.1 Results

Eliminating truncation from the model significantly increases the sensitivity of the parameters, even leaving the time constants with single possible values. However, it is physically preferable to have no truncation in the model, and the result obtained with the new parameters after the elimination of the linear trends and truncation introduced by Paillard proves the model is still able to correctly simulate the problematic stage 11 and the 100 kyr periodicity (Figure 3.7). Introduction of the continuous CO<sub>2</sub> then resulted in an improvement of only 2.2 % compared to the results obtained by Paillard, both models correctly placing the Mid-Pleistocene Transition between 1200 and 800 kyr ago while the model without any trends has a 100 kyr periodicity throughout the entire simulation. The most notable result was the  $v_{max}$  being strictly linear whilst it was allowed to fluctuate according to the CO<sub>2</sub> curve. This would have indicated the decreasing linear trend in CO<sub>2</sub>, the general cooling of the atmosphere, plays an important role in the MPT, but the fluctuations in CO<sub>2</sub> do not. It must also be noted that Paillard has a very large trend added directly to the insolation forcing (6 W m<sup>-2</sup> in 2 Myr) while the calculated  $\Delta R$  (Equation 2.6.1) only has a linear decrease of approximately 0.75 W m<sup>-2</sup> in 2 Myr (Figure 2.2), corresponding to a linear decrease in atmospheric CO<sub>2</sub> of approximately 20 ppm Myr<sup>-1</sup>. The large trend introduced by Paillard must be superfluous as we were able to produce the Mid-Pleistocene Transition with a much smaller trend added directly to the forcing.

Allowing linear or continuous trends in the insolation thresholds resulted in a constant  $i_1$ , a linearly decreasing  $i_0$  with a very small inverse relation to the fluctuations in CO<sub>2</sub> and, most importantly, significant fluctuations in the  $v_{max}$  threshold caused by the CO<sub>2</sub> curve. This could imply that the  $i_0$  and  $v_{max}$  thresholds are linked, which is understandable because they govern the transitions to and from the mild glacial, while the  $i_1$  threshold that determines the G - i transitions is independent of CO<sub>2</sub> and thus  $v_{max}$  and  $i_0$ . However, when atmospheric CO<sub>2</sub> decreases we should expect an increase instead of a decrease in the  $i_0$  threshold. The inception of a mild glacial should be able to occur at higher insolation values (at higher  $i_0$  values) because the temperature of the climate is already lower due to decreasing atmospheric CO<sub>2</sub> values, but the decreasing trend in the  $i_0$  threshold implies the model needs increasingly lower insolation values for the i - g transition to occur. The model thus requires both increasingly lower insolation values and lower temperatures for the inception of a mild glacial. This self-contradiction by the model, a statistically better result due to a non-physical trend, is a clear implication that this conceptual three-state model is improved more easily by improvements in specific glacial-interglacial cycles than by increasingly accurate physical representation.

The clear limitations of the model become apparent in the significantly increased sensitivity: slight changes in parameter values will now severely misplace certain glacial-interglacial cycles. It appears that the sensitivity increases when the physical justifiability increases through elimination of truncation and incorporation of the continuous CO<sub>2</sub> curve. Moreover, as most of the changes in parameter values are highly localized, whilst the problematic stage 11 paradoxically appears the most stable cycle, we are unable to make hard statements about individual cycles with this kind of conceptual model.

## 4.2 Conclusion

The three-state model proposed by Paillard appears to be successful in simulating the 100 kyr-problem, the stage 11 problem and the Mid-Pleistocene Transition. In this research project we have reproduced the model and were able to obtain very similar results to those reported by Paillard. Furthermore, we have improved his model by removing the truncation of the insolation forcing and consistently using the same dataset, replacing the linear trends in the  $v_{max}$  threshold and insolation with a continuous CO<sub>2</sub> simulation curve, and adding CO<sub>2</sub>-dependent trends in the insolation thresholds  $i_0$  and  $i_1$ . We have demonstrated that indeed ‘*the geological record can easily be explained in the framework of the classical astronomical theory*’ (Paillard, 1998) and confirmed the research questions of this project by improving the accuracy of the model, decreasing the root mean square error with the reference ice volume by 7.7 %.

### 4.3 Further research

In this project we have consistently used the same dataset (Stap et al., 2016), utilizing the  $\text{CO}_2$ , sea level and insolation. But there are many other datasets with different interpretations of benthic oxygen isotopes and sea level. An example of different sea level curves is given in Figure 4.1 below.

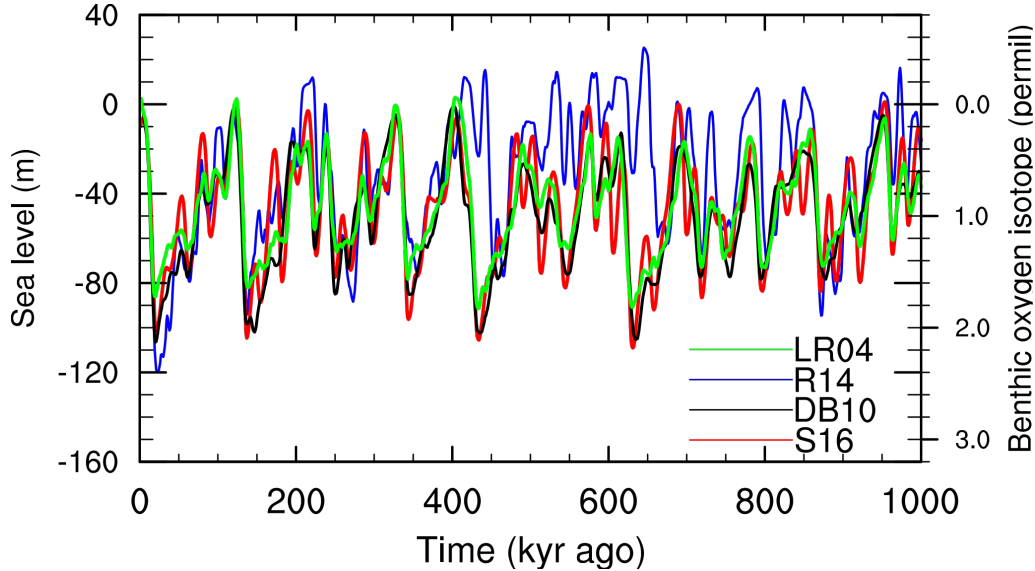


**Figure 4.1** – Different sea level curves. S16 (Stap et al., 2016) and DB10 (de Boer et al., 2010) are based on inverse decomposition of  $\delta^{18}\text{O}$  records (left axis). LR04 (Lisiecky and Raymo, 2005) and R14 (Rohling et al., 2014) are benthic oxygen records. S16 was used in this research project. Figure by L. Stap, 2016.

It is clear that the different sea level curves can vary significantly from one another. This can greatly influence the results because the sea level is used for the calculation of the reference ice volume. For example, the maximum at 50 kyrBP in S16 does not appear in the other curves and this maximum is consistently missed by our model results (Figures 3.8, 3.9 and 3.10), the curve being much more similar to the one of LR04 (Lisiecky and Raymo, 2005). The parameter values used in the final models of this research project are fully tuned to the S16 dataset and will most probably not work for other data. Tuning them to other datasets can therefore be very beneficial for the interpretation of the parameters and determining their role in future climate changes.

### 4.4 Acknowledgements

Thanks to Lennert Stap MSc for providing all data used in this research project, to Joel for helping me with LaTeX, to Gino for helping me with Python, to Emma for making the front page image and to my parents for encouragement and comments. Most of all thanks to dr. Roderik van de Wal for the great help and feedback throughout the entire project.





# Bibliography

- [1] Ashwin, P. and Ditlevsen, P.D.: ‘The middle Pleistocene transition as a generic bifurcation on a slow manifold’, *Climate Dynamics* 45: 2683-2695, 2015.
- [2] Berger, A.L.: ‘Long-term variations of daily insolation and Quaternary climatic changes’, *Journal of the Atmospheric Sciences* 35: 2362-2367, 1978.
- [3] Bintanja, R. and van de Wal, R.S.W.: ‘North American ice-sheet dynamics and the onset of 100,000-year glacial cycles’, *Nature* 454: 869-872, 2008.
- [4] de Boer, B., van de Wal, R.S.W., Bintanja, R., Lourens, L.J., Tuenter, E.: ‘Cenozoic global ice-volume and temperature simulations with 1-D ice-sheet models forced by benthic  $\delta^{18}\text{O}$  records’, *Annals of Glaciology* 51: 23-33, 2010.
- [5] Clark, P.U. and Pollard, D.: ‘Origin of the middle Pleistocene transition by ice sheet erosion of regolith’, *Paleoceanography* 13: 1-9, 1998.
- [6] Daruka, I. and Ditlevsen, P.D.: ‘A conceptual model for glacial cycles and the middle Pleistocene transition’, *Climate Dynamics* 46: 29-40, 2016.
- [7] Köhler, P., Bintantja, R., Fischer, H., Joos, F., Knutti, R., Lohmann, G., Masson-Delmotte, V.: ‘What caused Earth’s temperature variations during the last 800,000 years? Data-based evidence on radiative forcing and constraints on climate sensitivity’, *Quaternary Science Reviews* 29: 129-145, 2010.
- [8] Laskar, J.: ‘Chaotic motion of the solar system: A numerical estimate of the chaotic zones’, *Icarus* 88: 266-291, 1990.
- [9] Lisiecky, L.E. and Raymo, M.E.: ‘A Pliocene-Pleistocene stack of 57 globally distributed benthic  $\delta^{18}\text{O}$  records’, *Paleoceanography* 20: 1-17, 2005.
- [10] Muller, R.A. and MacDonald, G.J.: ‘Glacial cycles and orbital inclination’, *Nature* 377: 107-108, 1995.
- [11] Muller, R.A. and MacDonald, G.J.: *Ice Ages and Astronomical Causes*, Springer-Verlag London Ltd, 2000.
- [12] Paillard, D.: ‘The timing of Pleistocene glaciations from a simple multiple-state climate model’, *Nature* 391: 378-381, 1998.
- [13] Petrović, A.: ‘Revolution and Insolation: How Milutin Milanković has assembled the puzzle of the climate?’, *Scientific Technical Review* I.IX: 3-10, 2009.
- [14] Rohling, E., Foster, G., Grant, K., Marino, G., Roberts, A., Tamisiea, M., Williams, F.: ‘Sea-level and deep-sea-temperature variability over the past 5.3 million years’, *Nature* 508: 477-482, 2014.
- [15] Stap, L.B., de Boer, B., Ziegler, M., Bintanja, R., Lourens, L.J., van de Wal, R.S.W.: ‘CO<sub>2</sub> over the past 5 million years: Continuous simulation and new  $\delta^{11}\text{B}$ -based proxy data’, *Earth and Planetary Science Letters* 439: 1-10, 2016.



# Python

```

1  # -*- coding: utf-8 -*-
   #Main model loop

   #For-loop through normalized forcing-data
   for x in zerogemstd:
6
   #Differential equation for ice volume
     v_1 = v_0 + ((v_R - v_0)/t_R - x/t_F)

   #G-i transition, adjusting constants
11    if S == 0 and x > i1:
       S = 2
       t_R = t_i
       v_R = v_i

16   #i-g transition, adjusting constants
       else:
           if S == 2 and x < i0: #i-g
               S = 1
               t_R = t_g
21               v_R = v_g

   #g-G transition, adjusting constants
           if S == 1 and v_1 > vmaxcurve[tel]:
26               S = 0
               t_R = t_g
               v_R = v_G

   #Making lists of results
       sdata.append(S) #Model state
       vdata.append(v_1) #Ice volume
31       vrdata.append(v_R) #v_R

   #Resetting v_1 for differential equation
       v_0 = v_1
36   #Counting for usage of correct v_max(t)
       tel = tel + 1

```

**Listing 1** – Basic code for the three-state Paillard model.